

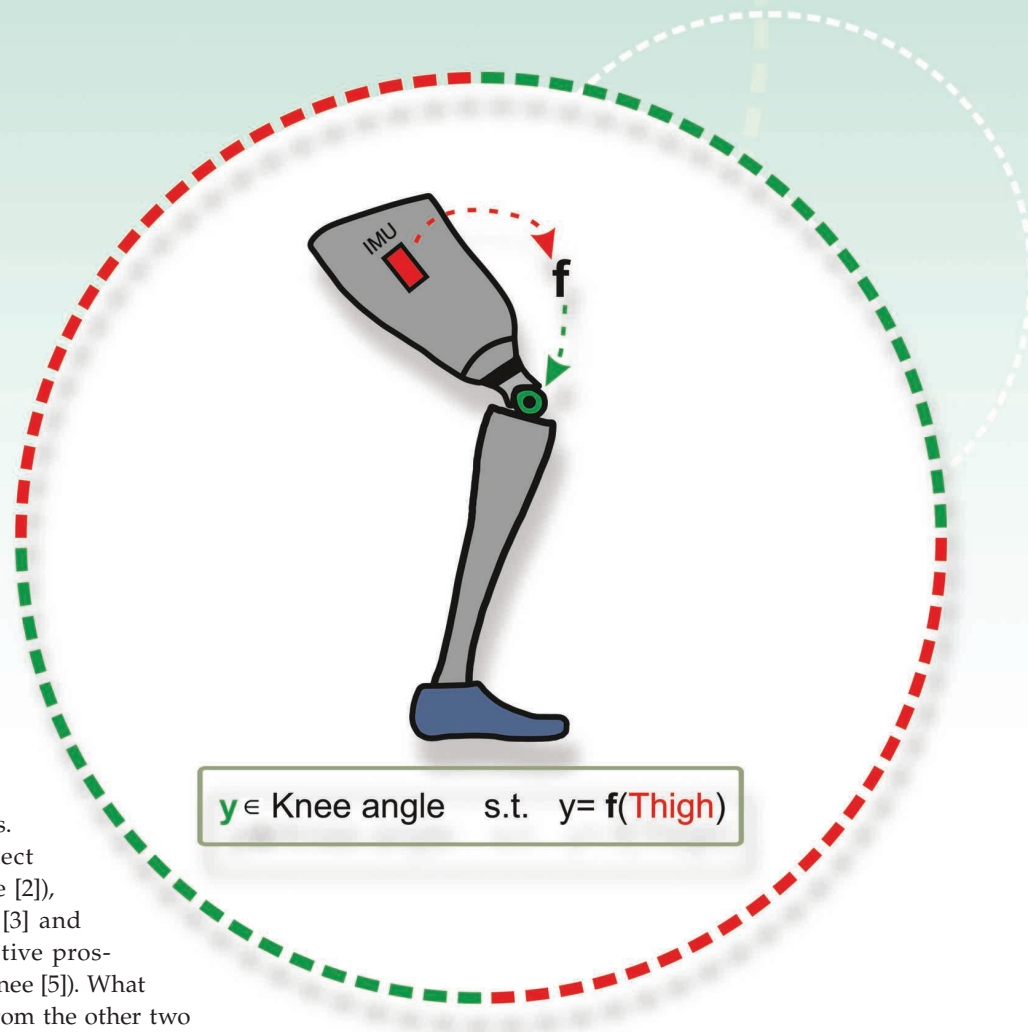
# Estimation of Knee Angles Based on Thigh Motion

A FUNCTIONAL APPROACH AND IMPLICATIONS FOR HIGH-LEVEL CONTROLLING OF ACTIVE PROSTHETIC KNEES

MAHDY ESLAMY,  
FELIX OSWALD, and  
ARNDT F. SCHILLING

**H**uman locomotion is the result of complex neuromusculoskeletal cooperation between different joints and limbs of the lower extremities. This collaboration (also called synergy [1]) results in an energy-efficient gait. Unfortunately, for an above-knee amputee, this cooperation is lost since current prosthetic devices do not emulate the missing functionality in a manner similar to their biological counterparts. Transfemoral amputees can select between passive (Mauch knee [2]), semi-active (Ottobock's C-leg [3] and Ossur's rheo knee [4]), and active prosthetic devices (Ossur's power knee [5]). What distinguishes the active ones from the other two is the injection of positive power for activities such as ascending stairs and standing up from a chair.

A major challenge that must be addressed to fully leverage the potential of active prosthetic knees is determining how to estimate the desired joint position in line with the actual motion of the person (see "Summary"). In an active prosthetic knee, the task of estimating the desired knee joint positions is implemented via a high-level controller [6] that determines the intention of



## Summary

A major challenge related to active prosthetic knees is how to estimate the desired joint positions in line with the actual motion of the amputee user. To tackle it, research is being devoted to finite-state-machine algorithms, which try to divide the gait cycle into different sections, with different control and area. Another approach, which is based on what we see in human locomotion, tries to see the gait cycle as a whole, regardless of speeds and gaits, if possible. This study is based on an even more challenging objective, that is, a seamless continuous-estimation algorithm. It uses machine-learning based Gaussian process regression to define a functional relationship  $y = f(x)$  that takes thigh angular velocities and angles (as inputs) and computes the knee joint positions (as outputs). The performance of the algorithm is tested on several subjects and for a wide range of walking speeds. The algorithm benefits from features such as requiring minimal inputs and being continuous; nevertheless, more investigations are required to find its limitations for use in active prosthetic knees.

the user and converts that information as a set-point input into the low-level controller [a proportional-derivative (PD) controller]. The low-level controller then combines this input with the actual motion of the prosthetic joint and other specific properties of the prosthesis (inertia and motor-torque limitations) to plan the desired trajectory and actuation to reach the goal set by the high-level controller. Knee joint positions are generally a function of the activity type (such as walking and running), speed, and gait phase (such as the heel strike, midstance, and toe-off). Furthermore, the general shape of knee joint diagrams varies for different people. Multiple solutions have been proposed by the research community to devise a high-level controller for prosthetic knees. A short review is presented next.

## CURRENT APPROACHES

### Replay From the Healthy Side

One of the first solutions to this problem was echo control [7], [8]. In it, the trajectories of the intact limb were replayed on the amputated side, taking into account the required time delay between the motions of the two sides. The main limitations were the intrinsic delay and the requirement to put sensors on the sound side. Complementary limb-motion estimation (CLME) and principal component analysis [9] (PCA) were used in [10] to extract couplings between the limbs of the healthy side and estimate the corresponding motion of the patient's affected joints. Unlike echo control [7], [8] (where the reference is a delayed replay of the sound leg's motion), CLME enables states to be instantaneously mapped.

### State-Machine Approach

Another common approach is based on the division of a gait cycle into different sections based on gait events (such as the heel strike, midstance, toe-off, and swing). This finite-state-machine approach was used to estimate the desired motion of the knee joint in a knee-ankle prosthesis during walking [11]. A single stride was divided into four distinct modes (finite states), as shown in Figure 1. The desired knee joint motions were regulated according to switching rules that were defined based on several sensory inputs from the ankle angle and torques, knee joints, and a load cell placed between the user and prosthesis to measure the interaction forces and moments. Within each state, the estimated desired knee motion was determined based on the impedance gains that were experimentally determined. A similar methodology was used in [12] to approximate desired knee motions in a powered transfemoral prosthesis while ascending and descending stairs. The finite-state approach was also used in [13] to regulate the knee operation in a powered knee prosthesis during walking. The gait cycle was divided into five states, and the transition criteria were defined based on the knee angle, angular velocity, and a load sensor.

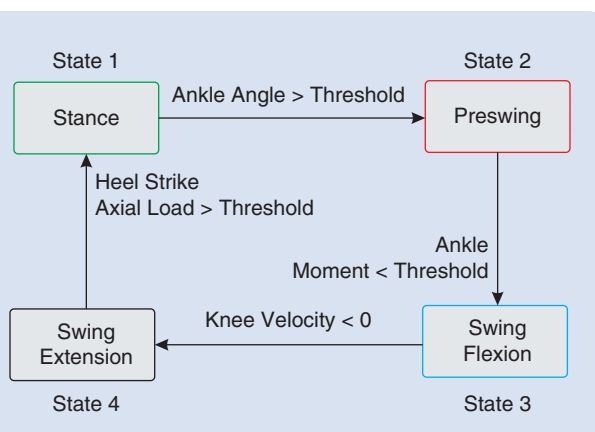


FIGURE 1 A finite-state approach (adapted from [11]).

### Continuous Approach

In contrast to the discrete methods (where a gait cycle is divided into states), a continuous method was proposed in [14] to estimate desired knee motions during walking on level ground and slopes with an active knee-ankle prosthesis. With this strategy, there was no need to divide a gait cycle into sections based on the gait events. Instead, the thigh angle and its integral were scaled and shifted to plot semicircular curves similar to [15], and a set of intermediate parameters was defined to compute a monotonic variable called the phase variable. Next, desired knee joint trajectories were predicted based on the virtual kinematic constraints and discrete Fourier transform. It was reported that controlling the prosthetic

## **Human locomotion is the result of complex neuromusculoskeletal cooperation between different joints and limbs of the lower extremities.**

device based on the residual thigh motion gave amputees control over the timing of the prosthetic joints.

PCA was used in [16] to determine the most important input parameters for an active knee and ankle prosthesis. Together with a Gaussian mixture model (GMM), different gait modes were recognized (standing and walking at 0.61, 0.78, and 0.94 m/s). The input signals were composed of knee and ankle positions and velocities, socket sagittal-plane moment, and heel- and ball-of-foot forces [16]. The GMM method was used in [17] to develop an estimator (high-level controller) for active knee prostheses. In [18], a GMM was employed to estimate desired knee positions in a lower-body exoskeleton using electroencephalography signals.

### **Approaches Based on Classification**

Electromyography (EMG) signals, together with ground-reaction forces, were used in [19] to classify the locomotion mode of transfemoral amputees wearing passive prosthetics. The EMG signals were recorded from gluteal and residual thigh muscles. The results suggested that the combined EMG and mechanical sensor fusion could outperform methods that incorporated only EMG [20] or mechanical sensory information to estimate the actual gait. In the study, support-vector machines were employed to classify the inputs corresponding to each locomotion type. In [21], EMG signals from eight hip muscles were used for terrain classification for an intelligent prosthetic knee. Several features (such as the mean absolute value and median power frequency) were extracted from the signals to classify locomotion on level ground and during ascent and descent on slopes and stairs. EMG signals were also harnessed to regulate joint impedance in a powered knee prosthesis [22]. The method utilized a combination of quadratic discriminant analysis and PCA to regulate the flexion/extension of the joint during sitting.

A dynamic Bayesian network was used in [23] as a classification strategy during level-ground walking and while ascending/descending stairs and ramps with a powered ankle-knee prosthesis. It was shown that by employing time history, steady-state misclassifications were reduced by more than half compared to other strategies. At the same time, the intent-recognition performance was not reduced during gait transitions. The sensors in that study included a six-axis inertial-measurement unit (IMU), an axial load sensor located on the middle of the shank, and the angular positions and velocities of the knee and ankle joints. The work was continued by incorporating the EMG

signals into previous mechanical-sensory information [24]. The results showed that the EMG information alone was not as accurate as mechanical-sensor information for classification. However, when the intent-recognition errors were significantly reduced, EMG information was combined with the mechanical-sensor information. Other methods that have been used to process or classify the sensory inputs in the context of active prosthetics are linear discriminant analysis [20], [25], neural networks [20], and  $k$ -nearest neighbors [26]. Model predictive control was used in [27] to estimate the joint motions (knee and hip) in an exoskeleton. The estimator required gait determinants, such as the step length, swing duration, and walking speed, to predict joint motions during the swing phase.

### **Limitations of Current Approaches**

As observed, the estimations related to the active prosthetic knees can be categorized based on different methodologies and inputs. Furthermore, the number and type of sensory inputs and the processing methods used to design the high-level controllers are different, and a clear standard does not exist. In one aspect, some of the previously mentioned methods focused on the classification of the gaits. However, regarding the estimation of the knee joint motion, employing only gait classification is insufficient. For example, when the gait type is determined through classification, the knee joint position is not only a function of that gait (such as walking, running, or ascending/descending stairs and slopes) but the speed and gait phase (such as the heel strike, midstance, and toe-off). Hence, classification (in the context of active prosthetics) requires further estimation steps. Nevertheless, classification seems necessary given that no estimation method in the literature to date has been suggested that can be used for several different human activities performed by the lower extremities (but not necessarily locomotion). According to the preceding discussion, an estimation algorithm that can provide the required desired joint motions within a gait cycle (at least for a determined gait and speed) would be advantageous.

From the viewpoint of the sensory inputs, the ideal scenario is that the estimation algorithm should require minimal sensory information [28]. EMG and mechanical sensors (angle positions, gyroscopes, and force) have been used for estimations, as reviewed. In [14], the proposed estimator incorporated a few sensory inputs (the thigh angle and its integral) to continuously provide desired motions for active

## Current prosthetic devices do not emulate the missing functionality in a manner similar to their biological counterparts.

prosthetic knees at different walking speeds and inclines. The integral was reset every gait cycle to prevent drift accumulation [14]. The phase-variable approach proposed in [28] also required the thigh angle and its integral but aimed to classify level walking and stair ascent and descent. To the best of our knowledge, the vast majority of the studies use more than two sensory inputs to estimate the desired joint positions.

From the perspective of estimation-algorithm continuity, more discrete methods have been proposed (where a gait cycle is divided into sections) than continuous estimators. Since the gait cycle seems to be a continuous process and not a succession of multiple discrete events [29], the state-machine approaches would be less attractive [14], [29] if a continuous estimator could be planned that does not need switching rules and states within a single stride [14].

### METHOD PROPOSED IN THIS STUDY

According to the previous discussions, the fundamental point of this article is to create a relationship between the motion of the knee joint and that of the thigh. Since the knee and thigh are in close proximity, creating a relationship between their motions would be very valuable for controlling active prosthetic knees. To accomplish this objective, the aim is to develop a continuous estimator for knee joint positions that can perform the task without requiring switching rules, speed classification, gait-percent identification, input data scaling, and shifting and lookup tables. It should also be able to do this with a minimum number of inputs.

The potential use of this estimator is to act as a high-level controller and provide desired knee joint positions for active prosthetic knees in line with a person's locomotion. This capability would enable continuous estimation of the knee joint positions (as outputs) with the thigh motion (as inputs) for a wide range of walking speeds (0.6–1.6 m/s). Furthermore, determining which input type (thigh angular velocity, thigh angle, or both) can help achieve such targets more accurately is also investigated. The estimation quality is studied for several scenarios encompassing a wide range of walking speeds, with data obtained from motion-capture cameras and IMUs. In addition, the strengths and limitations of the proposed estimator are evaluated through inter- and intrasubject testing scenarios and for extrapolation (when the estimator is trained for 0.6 and 0.9 m/s but should estimate the outputs for 1.2 m/s) and interpolation cases (when the estimator is

trained for 0.6, 0.9, and 1.4 m/s but should estimate the outputs for 1.2 m/s).

Similar to [14], this study aims to develop an estimator that can continuously predict knee joint positions within a gait cycle at different walking speeds. However, unlike [14], this is achieved without the need to scale/shift the input data or define a set of intermediate parameters for final estimations. The idea is to directly estimate the knee joint positions from the thigh motion through the minimum number of inputs. In addition, the goal is to develop an algorithm whose inputs could be obtained with little effort from a prosthetic device in real-world applications. For instance, IMUs are off-the-shelf sensory devices that can be easily embedded within a prosthetic device. Therefore, the selected inputs are the thigh angular velocities and angles.

We investigate the existence of a functional relationship [ $y = f(x)$ ] between the motion of the knee joint and that of the thigh. To achieve this target, Gaussian process (GP) regression [30] is used to seamlessly map thigh angular motion (as inputs) to knee joint positions (as outputs). It finds the relationship between the inputs and outputs based on probability theory and is a generalization of the Gaussian probability distribution [30].

In [31], GP regression was used to continuously predict the status of the missing limbs from intact limbs for a hand neuroprosthesis. GP regression was used in [32] to forecast trajectories for joint motions, in which the training inputs were 12 body parameters that estimated the angles of hip, knee, and ankle joints (as outputs). In [33], GP regression was harnessed to predict the skin temperature due to the use of lower-limb prostheses. GP regression was also used in [34] to introduce an adaptive-walking control method for active prosthetic feet. In that work, GP regression was implemented to predict power requirements as a function of gait percent and speed. The functional viewpoint was also considered in [1], in which an attempt was made to create a relationship between upper- and lower-extremity joints. To the best of our knowledge, regression has not been previously used for active prosthetic knees in a way that is similar to the one presented in this study.

### Applications of the Proposed Method

The estimator proposed in this study can be used to design high-level controllers for active prosthetic knees whose actuation mechanisms use a stiff spring [35] or no spring [36] since, in these cases, the trajectories of the motor positions will be similar to the knee joint positions. The outcome

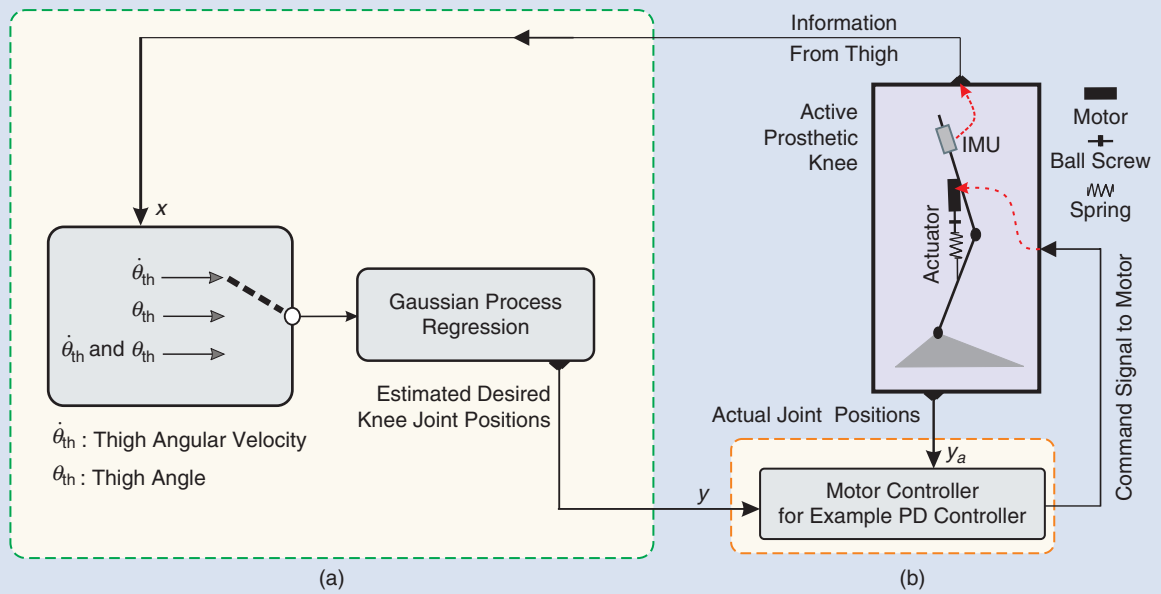


**FIGURE 2** An overall control structure for an active knee prosthesis/orthosis. (a) Estimator (high-level controller) and (b) low-level controller. A part of the acquired sensory information ( $x$ ) is used as inputs by the estimator, or high-level controller (a), to approximate the desired required knee joint positions  $y$ . The inputs can be the thigh angular velocity  $\dot{\theta}_{th}$ , thigh angle  $\theta_{th}$ , or both  $[\dot{\theta}_{th}, \theta_{th}]$ . The effect of each input type on the quality of the estimations will be discussed in detail in this study. (b) Additionally, a part of the sensory data is used to create the required command signal through the low-level controller [or the motor controller (b)] to actuate the prosthetic device. As observed, for the low-level controller to be operative, it requires the output of the estimator (or the high-level controller). Different actuation mechanisms can be used for active prosthetic knees [35], [37]. Here, an example is shown with a motor and a spring in series. The “Method” section contains detailed information in this regard. This study addresses part (a). IMU: inertial measurement unit; PD: proportional-derivative.

of the estimator can be used by a low-level controller to actuate the prosthesis accordingly. In [37]–[40], detailed discussions of how to design such motor (actuator) trajectories are available.

## METHOD

### Fundamentals and Basic Definitions

In Figure 2, the overall scheme for the control structure of an active prosthetic knee is illustrated. Figure 2(a) shows the estimator that receives thigh motion data ( $x$ ) and approximates the corresponding desired knee joint positions  $y$ . As previously mentioned, in the context of active prosthetics, the estimator is also called the high-level controller [6]. Figure 2(b) describes the low-level controller, or motor controller, that processes the estimated desired joint positions  $y$  and the actual ones  $y_a$  (from embedded sensors) to create the error signal and produce the command signal for the motor. This objective can be achieved through well-established controllers, such as impedance and PD controllers. In Figure 2, for the controller in (b) to be operative, the estimator in (a) is an absolute requirement. This study concentrates on Figure 2(a).

As seen in Figure 2, the inputs could be the thigh angular velocity  $\dot{\theta}_{th}$  or thigh angle  $\theta_{th}$ . In addition, it is possible to make a combined input as  $x = [\dot{\theta}_{th}, \theta_{th}]$ . The

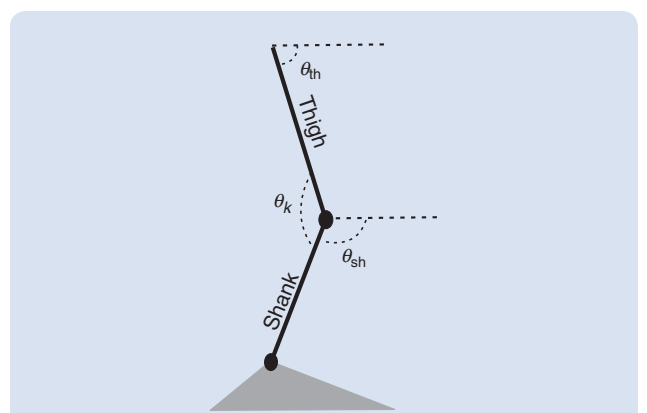


**FIGURE 3** The definition of the thigh and shank angles ( $\theta_{th}$  and  $\theta_{sh}$ ) and knee joint positions ( $\theta_k$ ). Note that shank angles are not required for estimations. However, as explained in the “Results and Discussions” section, during experiments with inertial measurement units, shank angles were used to indirectly calculate the knee angles.

effect of each input type on the estimation quality will be investigated in detail in the “Results and Discussions” section. Figure 3 gives the definitions of thigh and knee angles ( $\theta_{th}$  and  $\theta_k$ ). The definition of shank angle  $\theta_{sh}$  is also shown, since it will be used later. More details will be provided in the “Results and Discussions” section

**TABLE 1** Data obtained via motion-capture cameras. The subjects' characteristics were used to obtain kinematics and kinetics data [41] (mean  $\pm$  standard deviation).

Number of Subjects	Age (Years)	Body Height (m)	Body Mass (kg)	Speeds (m/s)
21	25.4	1.73	70.9	Walking
	$\pm 2.7$	$\pm 0.09$	$\pm 11.7$	0.5, 1, 1.5

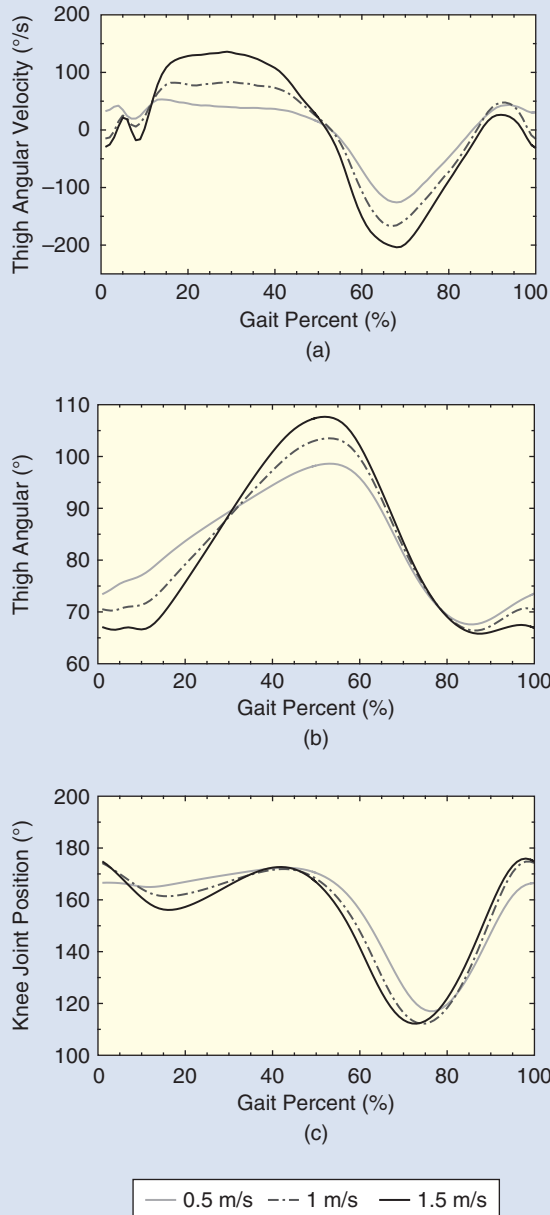


**FIGURE 4** (a) Thigh angular velocity ( $\dot{\theta}_k$ ). (b) Thigh angle ( $\theta_{th}$ ). (c) The expected knee joint positions desired for walking 0.5, 1, and 1.5 m/s. The diagrams show the mean data for 21 subjects [41]. The data were obtained via motion-capture cameras.

when IMU data are used to evaluate the estimation quality. It should be noted that the estimation algorithm does not require shank angles.

Part of this study uses data obtained from 21 subjects [41] in a laboratory environment equipped with motion-capture cameras (Qualisys, Gothenburg, Sweden) and an instrumented treadmill (type ADAL-WR, HEF Tecmachine, Andrezieux Boutheon, France). The data were for walking 0.5, 1, and 1.5 m/s [41], and general information about the subjects can be seen in Table 1. For each subject and speed, at least 21 walking cycles were used to obtain the mean data [41]. The subjects were divided into training and test groups, as explained in the "Results and Discussions" section when different testing scenarios are defined. In Figure 4, (a) and (b) provide diagrams of thigh angular velocities and thigh angles for those speeds, respectively (mean of 21 subjects).

In human biomechanics, the gait cycle starts with the heel contact and ends with the next contact of the same foot. In this study, a gait cycle is divided into 100 sections, which is called the gait percent [42]. As observed in Figure 4(c), for each speed and gait percent, a corresponding expected knee joint position exists. The expected knee joint positions were obtained using motion-capture cameras [41] (for the 21 subjects) or IMUs (for another two subjects), as explained in the "Results and Discussions" section. The expected knee joint positions are required for comparison with the estimated desired knee positions  $y$  (which will be the output of the high-level controller). The task of the high-level controller is to estimate an acceptable knee joint position corresponding to each input ( $[\dot{\theta}_{th}], [\theta_{th}]$ , or  $[\dot{\theta}_{th}, \theta_{th}]$ ).

### Gaussian Process Regression-Based High-Level Controller

In this study, the problem of developing the high-level controller is converted into the problem of finding an appropriate function  $f$  that can map the inputs  $x$  to the outputs  $y$ . The proposed high-level controller is based on the synergy (cooperation and collaboration) between the motion of the thigh and that of the knee, and it creates a connection between the motion of the thigh as input  $x$  and the motion of the knee as output  $y$ . From a functional point of view, this can be stated as  $y = f(x)$ .

GP regression [30] was used to define function  $f$ . Regression, in general, estimates continuous quantities (in this article, knee joint positions  $y$ ). The goal is to make inferences about the relationship between the inputs  $x$  (the thigh angular velocity and angle) and outputs  $y$  (knee joint positions). Furthermore, GP regression aims to learn a function  $f$  that can be used to estimate outputs for the new (unseen) test inputs [30], [43].

A GP is defined by its mean  $m(x)$  and the covariance function  $k(x, x')$  for the input pair  $x$  and  $x'$  as [30]

$$f(x) \sim \mathcal{GP}(m(x), k(x, x')), \quad (1)$$

where  $m(x) = E[f(x)]$  [ $E$  denotes the expectation of  $f(x)$ ] and  $k(x, x') = E[(f(x) - m(x))(f(x') - m(x'))]$ . Some a priori training is required to use GP regression for prediction [30]. The input training set could be  $[\dot{\theta}_{\text{th}}, \theta_{\text{th}}]$ , or  $[\dot{\theta}_{\text{th}}, \theta_{\text{th}}]$ , and it can be formed as  $D = \{(x_i, f_i) | i = 1, \dots, n\}$ , where index  $i$  shows every (input) item out of 100 for each speed under investigation. Consequently, for three speeds, there would be 300 items (since a gait cycle is divided into 100 sections: the gait percent [42]). Therefore,  $D$  consists of  $n$  observations, where  $x_i$  is a  $d$ -dimensional row vector, depending on whether one type of input ( $[\dot{\theta}_{\text{th}}]$  or  $[\theta_{\text{th}}]$ ) or two ( $[\dot{\theta}_{\text{th}}, \theta_{\text{th}}]$ ) is used, and  $f_i$  is the corresponding function (output) value. In other words,  $y_i = f(x_i)$ . The effect of each input type on the estimation quality is discussed in detail in the “Results and Discussions” section.

In addition, concatenating the training observations will form the aggregated input matrix  $x$  as

$$x = \begin{pmatrix} x_1 \\ x_2 \\ x_3 \\ \vdots \\ x_n \end{pmatrix}, \quad y = f = \begin{pmatrix} y_1 \\ y_2 \\ y_3 \\ \vdots \\ y_n \end{pmatrix}. \quad (2)$$

A test set is also required to evaluate the prediction performance of GP regression. The test inputs are denoted as  $x^*$ . Accordingly, the outputs related to  $x^*$  are marked as  $f^*$  [or  $y^* = f^*(x^*)$ ]. Inputs close to each other should logically have quite similar output values (since the output is a continuous bounded function). Therefore, training inputs that are close to the test inputs should be logically informative for prediction. In GP regression, the covariance function  $k$  defines such a similarity. The covariance function is also a designer-defined parameter. GP regression is able to handle different covariance functions. A full list can be found in [30] and [43]. In this study, different covariance functions were investigated (not all are shown), and the best estimation quality was observed when the Matérn covariance function was used.

The Matérn class of covariance function is in the form of

$$k_{\text{Matérn}}(r) = \frac{2^{1-\nu}}{\Gamma(\nu)} \left( \frac{\sqrt{2\nu} r}{l} \right)^{\nu} K_{\nu} \left( \frac{\sqrt{2\nu} r}{l} \right), \quad (3)$$

where  $r$  is the absolute difference of input pairs  $x$  and  $x'$  ( $r = |x - x'|$ ), and  $\nu$  and  $l$  are positive parameters called hyperparameters  $\Theta$ , where  $K_{\nu}$  is a modified Bessel function [30].

One common approach to determine the hyperparameters  $\Theta$  is to maximize the log marginal likelihood [30], [43], which is expressed as

$$\log p(y|x, \Theta) = -\frac{1}{2} (y^T K(x, x) y + \log|K(x, x)| + n \log 2\pi), \quad (4)$$

where  $p(A|B)$  is the conditional probability of A, given that event B is true [30]. The first term of (4) addresses the data

fit, the second introduces a complexity penalty, and the last is a normalization constant [30], [43]. The log marginal likelihood automatically performs a tradeoff between the model fit and complexity. Several optimization algorithms exist for this purpose [30], [43]. In this study, hyperparameters were optimized through the exact inference method together with the Gaussian likelihood since the best estimation results were obtained by using those methods.

The joint distribution of the training outputs  $f$  and the test outputs  $f^*$  is [30]

$$\begin{bmatrix} f \\ f^* \end{bmatrix} \sim \mathcal{N} \left( 0, \begin{bmatrix} K(x, x) & K(x, x^*) \\ K(x^*, x) & K(x^*, x^*) \end{bmatrix} \right), \quad (5)$$

where  $K(x, x^*)$  is the  $n \times n^*$  matrix of the covariances evaluated at all pairs of training and test points. A  $K(x, x)$  is defined as

$$K(x, x) = \begin{pmatrix} k(x_1, x_1) & k(x_1, x_2) & \dots & k(x_1, x_n) \\ k(x_2, x_1) & k(x_2, x_2) & \dots & k(x_2, x_n) \\ \vdots & \vdots & \ddots & \vdots \\ k(x_n, x_1) & k(x_n, x_2) & \dots & k(x_n, x_n) \end{pmatrix}. \quad (6)$$

A similar statement can be expected for other  $K(., .)$ .  $\mathcal{N}$  denotes the normal distribution.

Given (5), it is possible to obtain information for  $f^*$  on the condition of having  $x, f$ , and  $x^*$  [30] as

$$f^*|x, f, x^* \sim \mathcal{N}(\bar{f}^*, \text{cov}(f^*)), \quad (7a)$$

$$\bar{f}^* = K(x^*, x) K(x, x)^{-1} f, \quad (7b)$$

$$\text{cov}(f^*) = K(x^*, x^*) - K(x^*, x) K(x, x)^{-1} K(x, x^*), \quad (7c)$$

where  $\bar{f}^*$  and  $\text{cov}(f^*)$  are the GP posterior mean and GP posterior covariance, respectively [30]. Equation (7) provides the solution for  $f^*$  to estimate the desired motor positions associated with the unseen new inputs (that is, the test inputs  $x^*$ ). It is also possible at this stage, if needed, to use smoothing algorithms (a moving average) to reduce sharp changes. In the following, the strengths and limitations of the proposed estimator (high-level controller) will be investigated in different scenarios.

## RESULTS AND DISCUSSIONS

### Effect of the Input Type on the Estimation Quality

We investigated how input types influence estimation quality. Therefore, the estimation quality was first evaluated using minimal inputs, that is, the inputs consisted of only the thigh angular velocities  $\dot{\theta}_{\text{th}}$  or thigh angles  $\theta_{\text{th}}$ . Next, the estimation quality was examined when both inputs  $[\dot{\theta}_{\text{th}}, \theta_{\text{th}}]$  were used.

### Acceptance Criterion

As mentioned, GP regression requires training and test groups, which are described for each scenario. To evaluate

## Estimations related to the active prosthetic knees can be categorized based on different methodologies and inputs.

the estimation quality, we employed root-mean-square (RMS) errors, mean absolute deviations (MADs), maximum absolute errors, and commonly used  $R^2$  values. These measures were employed in previous studies [44]–[46].

To the best of our knowledge, there is no gold standard for determining which estimation results should be deemed acceptable for active prosthetics. We used the same criterion as [46] for the acceptable estimation quality. In that study,  $R^2$  values higher than 0.8 were a sign of acceptable estimations (the maximum is one). Nevertheless, there are studies in which the experimental  $R^2$  values are less than that threshold [34], and those experiments were conducted with satisfactory performance. However, to submit our results to a more challenging rule, we used  $R^2$  values higher than 0.8 for an acceptable estimation. Therefore, for each of the following scenarios, we used this definition to decide whether the estimation quality was acceptable or not. Accordingly, in the tables,  $R^2$  values lower than 0.8 are underlined and denoted by an “x,” indicating unsatisfactory results.

### **Single Input: Thigh Angular Velocity or Thigh Angle**

Initially, the training and test inputs consisted of the thigh angular velocities  $\dot{\theta}_{th}$  for walking 0.5, 1, and 1.5 m/s. The 21 subjects were randomly divided into a training group (10 subjects) and a test group (11 subjects). The mean  $R^2$  values for the 11 subjects were 0.62, 0.6, and 0.42 for 0.5, 1, and 1.5 m/s, respectively, and therefore not acceptable according to the criterion ( $R^2 < 0.8$ ). Next, the training and test inputs consisted of the thigh angles  $\theta_{th}$  with the same training and testing procedure. Again, the  $R^2$  values were

not acceptable since the mean values for the 11 subjects were 0.04, 0.27, and 0.43 for 0.5, 1, and 1.5 m/s, respectively.

One possible reason for such results could be the relationship between the thigh angular velocity or angle and the expected knee joint position. For each thigh angular velocity or thigh angle, (at least) two values of expected knee joint positions can be obtained [Figure 5(a) and (b)]. In contrast, Figure 5(c) shows that there are approximately no points that have similar  $[\dot{\theta}_{th}, \theta_{th}]$  and different expected knee joint positions. Therefore, the investigations are extended to double-input scenarios, where thigh angular velocities and thigh angles are used.

### **Double Input: Thigh Angular Velocity and Angle**

We first concentrated on the data obtained via motion-capture cameras. To investigate the estimation quality for the double-input case (where the inputs are  $[\dot{\theta}_{th}, \theta_{th}]$ ), the leave- $p$ -out scenario ( $p = 1$ ) was used. One subject was used as test group, and the data for the remaining 20 subjects were employed for training. That was done for all 21 subjects under investigation (scenario A). The results for the RMS errors, MADs, maximum absolute errors, and  $R^2$  values are shown in Figure 6.

The inputs for scenario A consisted of the raw unfiltered input data. In scenario B, Kalman-filtered inputs were used [see Figure 4(a)]. The curve for the thigh angular velocity was not smooth enough at some sections of the gait cycle. Filtering was performed to slightly smooth the input data (the process was similar in all the procedures) without concentrating on obtaining the best optimal estimation for any of the test subjects. When the filtered inputs were used, the

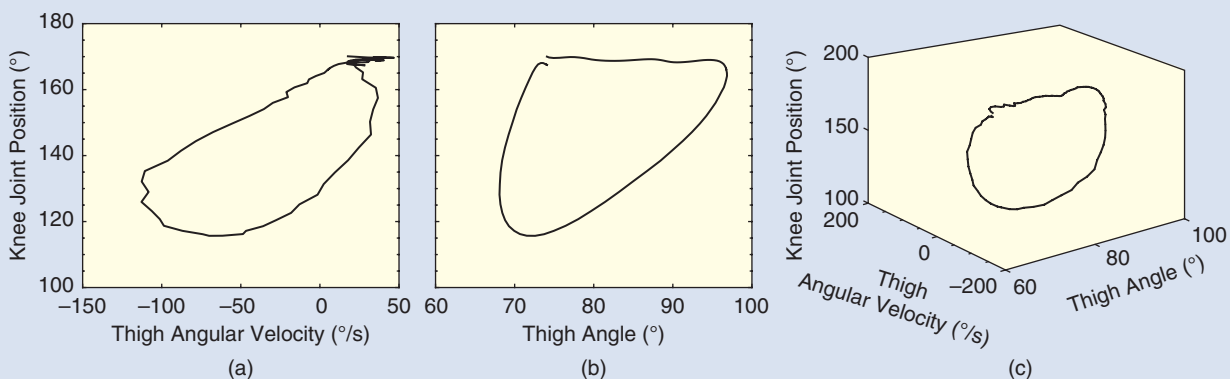


**FIGURE 5** The diagrams of the knee joint positions with respect to (a) thigh angular velocity  $\dot{\theta}_{th}$ , (b) thigh angle  $\theta_{th}$ , and (c)  $[\dot{\theta}_{th}, \theta_{th}]$ . The graphs show the results for one test subject in scenario A, walking 0.5 m/s.

estimation quality increased. For a better comparison, the results of this scenario are shown in Figure 6 along with those of scenario A.

### **Estimator Evaluation With Inertial Measurement Units**

For a real-world active prosthetic knee, IMUs are typically embedded in the device. In this section, the performance of the estimator is evaluated through the data obtained from IMUs. Two IMUs (MTw Awinda, Xsens Technologies, The Netherlands) were attached to the thigh and shank of two male participants (subject 1: 61 kg, 1.71 m; subject 2: 86 kg, 1.77 m) walking at speeds of 0.6, 0.9, 1.2, 1.4, and 1.6 m/s on a treadmill. The subjects were different from the other 21, and the experiments were performed in another lab. The thigh angular velocity, thigh angle, and shank angle ( $\theta_{sh}$ ) were obtained during the experiments. Although the

estimator needs only one thigh IMU, two IMUs were used so that we could calculate the corresponding knee joint positions  $\theta_k$  indirectly from the measured thigh and shank angles after the experiments. The definition of the knee joint positions  $\theta_k$  is illustrated in Figure 3 according to  $\theta_k = 180 - (\theta_{sh} - \theta_{th})$ . As mentioned, we need to know the expected knee joint positions for comparison with the estimated knee positions. Based on the obtained data, the following investigations were performed. As before, the training and test inputs were  $[\dot{\theta}_{th}, \theta_{th}]$ .

### **Scenario C**

The training data were for walking at 0.5, 1, and 1.5 m/s (from motion-capture cameras), and the test inputs were for walking 0.6, 0.9, 1.2, 1.4, and 1.6 m/s (IMU data). The training group was composed of five randomly selected subjects from the

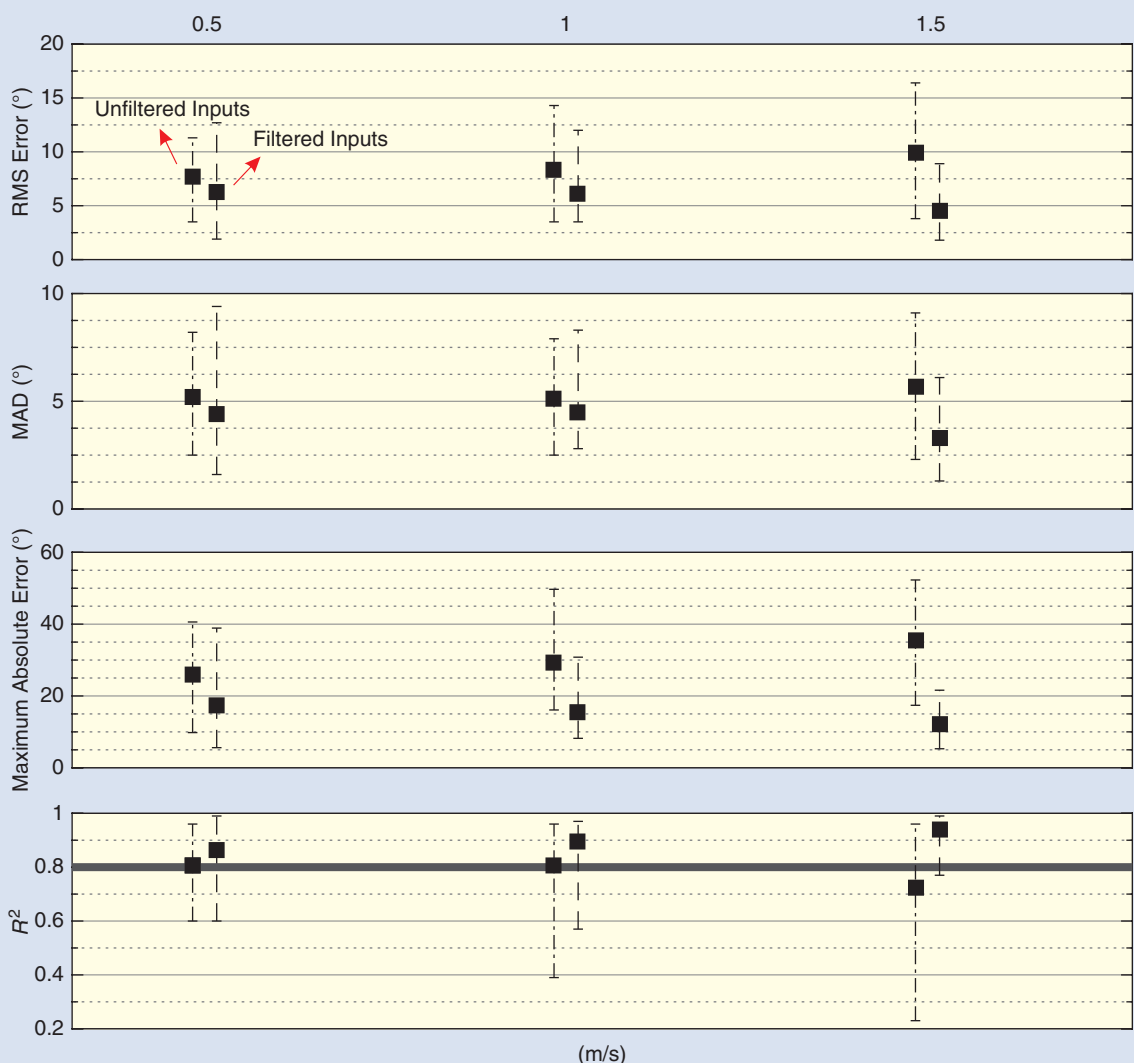


**FIGURE 6** The results for the leave- $p$ -out scenarios ( $p=1$ ; scenarios A and B). The black squares show the average. The range of root-mean-square (RMS) errors, mean absolute deviations (MADs), maximum absolute errors, and  $R^2$  values are presented for walking at 0.5, 1, and 1.5 m/s.

## The gait cycle seems to be a continuous process and not a succession of multiple discrete events.

group of 21, and test subject 1 was included with IMU data (as explained previously). The RMS errors, MADs, maximum absolute errors, and  $R^2$  values are presented in Table 2. The results are the mean of 13 consecutive gait cycles for subject 1. This scenario was conducted to evaluate the performance of the estimation algorithm when the testing speeds differed from the training speeds. Observed data from motion-capture cameras were used to evaluate the information from the IMUs, and the robustness of the algorithm was simultaneously verified through intersubject testing.

### Scenario D

The training data were for walking 0.6 m/s, and the test inputs were for walking 0.9, 1.2, 1.4, and 1.6 m/s (all from subject 1). In this case, intrasubject extrapolation testing was performed (that is, when the test speeds varied from the training speeds). The results are presented in Table 3 and show the mean of 13 consecutive gait cycles.

### Scenario E

The training data were for walking 0.6 and 0.9 m/s, and the test data were for walking 1.2, 1.4, and 1.6 m/s (subject 1). The results are presented in Table 4 and convey the mean of 13 consecutive gait cycles. This scenario was similar to the previous one. However, more training speeds were used to verify the estimation-quality change.

**TABLE 2** The results according to scenario C.

Gait Type		Walking				
Speed (m/s)	0.6	0.9	1.2	1.4	1.6	
Root-mean-square error (°)	9.3	9.9	7.8	5.2	8.7	
Mean absolute deviation (°)	7.2	8.3	5.7	3.8	7	
Maximum absolute error (°)	20.2	20	17.2	13.8	21.5	
$R^2$	0.81	0.81	0.84	0.94	0.81	

**TABLE 3** The results according to scenario D.  $R^2$  values lower than 0.8 are underlined and denoted by an “x.”

Gait Type		Walking				
Speed (m/s)	0.9	1.2	1.4	1.6		
Root-mean-square error (°)	4.5	8.6	8.2	12.6		
Mean absolute deviation (°)	3.7	7.9	7.4	11.4		
Maximum absolute error (°)	11.2	15.1	14	20.41		
$R^2$	0.96	0.8	0.85	<u>0.6</u> <sup>x</sup>		

### Scenario F

The training data were for walking 0.6 and 1.6 m/s, and the test data were for walking at 0.9, 1.2, and 1.4 m/s (subject 1). In this case, the intrasubject interpolation capability of the estimator was under investigation (that is, when the test speeds were within the range of the training speeds but not exactly the same). The results are reported in Table 5, showing the mean of 13 consecutive gait cycles.

### Scenario G

The training data were for subject 1 walking at 0.6, 0.9, 1.2, 1.4, and 1.6 m/s. The test inputs were for subject 2 at the same speeds. Therefore, an intersubject test with IMU data was performed. The results are presented in Table 6 and give the mean of 13 consecutive gait cycles for subject 2.

### Discussion

In scenario A (where raw unfiltered inputs were used for the training process), the average  $R^2$  values were near 0.8 for 0.5 and 1 m/s; for 1.5 m/s, the value was slightly above 0.7. According to the acceptance criterion, the results could not be deemed acceptable for 1.5 m/s. However, when filtered inputs were used (scenario B), the average  $R^2$  values increased for all speeds. This showed that input irregularities can reduce the quality of the estimations. The filtering

**TABLE 4** The results according to scenario E.

Gait Type		Walking		
Speed (m/s)		1.2	1.4	1.6
Root-mean-square error (°)		8.1	5.7	7.5
Mean absolute deviation (°)		6.4	4.7	6
Maximum absolute error (°)		22	13.1	15.7
$R^2$		0.82	0.93	0.86

**TABLE 5** The results according to scenario F.

Gait Type		Walking		
Speed (m/s)		0.9	1.2	1.4
Root-mean-square error (°)		6.6	4.2	5
Mean absolute deviation (°)		5.2	3.1	4
Maximum absolute error (°)		14.6	10.9	11.9
$R^2$		0.91	0.95	0.94

## Although it is obvious that ideal results must be perfect, it is not clear to what extent deviations are acceptable and allowed.

was similar for all procedures, with no intention to obtain the best possible estimation for any of the test subjects. In this way, we tested the generality of the procedure and the estimation quality. This study could be continued by evaluating how much filtering can improve and optimize the estimation quality.

In scenario C, where the training inputs came from motion-capture cameras and the test inputs were obtained from IMUs (as observed in Table 2, for 0.6, 0.9, and 1.6 m/s), the  $R^2$  results were, surprisingly, still slightly higher than the minimum success criterion. This was the case in which the training and test data were obtained from two experimental procedures (motion-capture cameras versus IMU sensors from different labs) and for various speeds, which shows the general robustness of the algorithm.

Based on the results from scenario C, the investigation was continued to consider the susceptibility of the estimator when tested for the speeds it was not trained for and were out of the training volume. To conduct this extrapolation test, in scenario D, the estimator was trained with the inputs from 0.6-m/s walking and tested for 0.9, 1.2, 1.4, and 1.6 m/s (all the inputs were from subject 1). As observed in Table 3, for the speed of 0.9 m/s, the estimation quality was acceptable. However, for 1.6 m/s, the estimation quality dropped below the acceptable threshold, thus showing the extrapolation limitations of the algorithm.

In scenario E, the extrapolation capability of the estimator was investigated further for the case in which training was performed with 0.6 and 0.9 m/s, and the testing was performed with 1.2, 1.4, and 1.6 m/s (all the inputs were from subject 1). With this training approach, all the  $R^2$  values were acceptable (Table 4), showing again that the algorithm is dependent on the level of the training regarding extrapolation scenarios.

In scenario F, the interpolation capability of the estimator was investigated. To conduct this case, the training was performed with 0.6 and 1.6 m/s, and the testing was performed with 1.2, 1.4, and 1.6 m/s. As seen in Table 5, the  $R^2$

values were acceptable and higher than the results related to extrapolation (scenarios D and E). In scenario G, the intersubject capability of the estimator was examined for IMU data. As seen in Table 6, the  $R^2$  values were acceptable for all speeds.

## CONCLUSION AND SUGGESTIONS

The findings in this study suggest that the cooperation, or synergy, between thigh motion and knee motion can be used to continuously map the thigh motion to the knee joint motion. This objective was achieved without the need to determine the speed, identify the gait percent, shift/scale the input data, or use lookup tables and switching rules, at least for the walking gait. Data from motion-capture cameras and IMUs were used to evaluate the strengths and limitations of the estimator. The estimator showed accuracy and potential that might warrant its use in active prosthetic knees. However, there are a number of points and limitations that might need further investigation.

### Estimation Quality

While the estimation quality of our algorithm was acceptable for most of the studied scenarios, in some cases there were obvious deviations in single parameters. As an example, in Figure 6, the maximum absolute error for 0.5 m/s can reach 40°, even though the overall mean  $R^2$  value is in the acceptable range. This might not be very desirable and shows that concentrating only on  $R^2$  values could be insufficient, as in [46]. This issue necessitates fundamental and continuous discussion in the research community about how a success criterion should be defined. Although it is obvious that ideal results must be perfect, it is not clear to what extent deviations are acceptable and allowed. Therefore, the absence of an acceptable success criterion that can describe the quality of the estimations is noticeable. Furthermore, it is still an open, challenging question regarding how to simultaneously take RMS errors, MADs, maximum absolute errors, and  $R^2$  values into account when defining the success of an algorithm.

Alternatively, patients are able to walk with passive devices that, to a great extent, do not emulate the functionality of human joints. In current prosthetics, even when obvious deviation between the commanded and performed trajectories is visible (as an example, compare the commanded and actual knee positions in [14]), experiments were apparently conducted without critical problems for the users. The experimental  $R^2$  values in [34] were below the threshold used in this study; however, it appears that

**TABLE 6** The results according to scenario G.

Gait Type	Walking				
	0.6	0.9	1.2	1.4	1.6
Speed (m/s)	0.6	0.9	1.2	1.4	1.6
Root-mean-square error (°)	6	5.4	6.3	7.1	7
Mean absolute deviation (°)	5	4.4	5.1	6.1	5.8
Maximum absolute error (°)	12	13	13.6	14.6	17
$R^2$	0.89	0.92	0.89	0.89	0.88

## The issue of whether or not prostheses move as expected from the user's perspective has not been clearly reported in the literature.

the experiments were performed with satisfactory performance for the patient. Therefore, it may be challenging to define how much deviation is acceptable and whether it truly presents a critical issue. Unfortunately, so far, the issue of whether or not prostheses move as expected from the user's perspective has not been clearly reported in the literature. These matters might enforce the use of criteria that concentrate not only on the kinematics (as we and many other studies have done) but on other criteria, such as metabolism and measurements of brain activities as well as how the person feels. As observed, the establishment of a well-defined criterion for the acceptance of the estimation quality is a challenging task and requires further investigation.

### Sensitivity to the Level of Training

Our study results showed that the algorithm can be sensitive to the level of training for extrapolation cases (scenarios D and E as shown in Tables 3 and 4). Specifically, this might cause problems when the algorithm is going to be used for speeds and gaits outside the training volume and if unexpected obstacles/perturbations occur. On the other hand, a lack of acceptable functioning outside the training volume might not be due to the algorithm but possibly to the type and number of the inputs. For instance, if EMG signals are used with kinematic ones, the estimator might work much better for new gaits/speeds that are outside the training volume and/or for transition cases, such as from level walking to stairs and vice versa. These matters require more investigation in the continuation of this study.

### Toward Biomimetic Neuromuscular Control of Prostheses

A common goal in prosthetics is to replace the lost functionality as well as possible. Ideally, the target is to have a device that the patient can use without thinking about it and that ultimately feels it like a part of herself/himself. In this study, we used thigh motion for inputs to the estimator. In this way, for application in prosthetic knees, estimating the desired motion of the prosthetic joint would be based on the motions of the remaining joints and limbs (that is, thigh motion) that are controlled by the user's biological nervous system. Such an attitude was also used in [14] for an active knee prosthesis and in [15] for an active ankle prosthesis.

The usefulness of active prostheses will depend on how patients feel toward them and whether the control algorithms provide patients with a feeling of command and integration during locomotion. The actuation design also plays a critical role in the final success of an active prosthetic. This will have

to be clarified with clinical evaluations of novel control concepts in the future.

### ACKNOWLEDGMENTS

Experiments to obtain data for this study were conducted at the Lauflabor Laboratory, Technical University of Darmstadt, Germany, for which the authors would like to express their gratitude. This work was partially supported by a grant from the Bundesministerium für Bildung und Forschung (INOPRO-16SV7656).

### AUTHOR INFORMATION

**Mahdy Eslamy** (mahdy.eslamy@med.uni-goettingen.de) received the B.S. degree from the Iran University of Science and Technology, Tehran, the M.S. degree from the Khajeh Nasir Toosi University of Technology, Tehran, and the Ph.D. degree in Germany, all in mechanical engineering. His research interests include biomechanics, design (dynamics/finite element analysis), control, and motion analysis. He received the prestigious Iranian Elites Foundation's grant and works in close cooperation with the University of Tehran. He currently conducts research and supervises students at the Applied Rehabilitation Technology lab, Medical University of Göttingen, Germany.

**Felix Oswald** received the B.S. degree in orthobionics. His research interests include human-movement analysis of the lower and upper extremities.

**Arndt F. Schilling** is a medical doctor and molecular biologist. He held professorships in biomaterial research and experimental plastic surgery at the Hamburg University of Technology, Germany, and the Technical University of Munich. He leads research and development at the Clinic of Trauma Surgery, Orthopedics, and Plastic Surgery at University Medical Center Göttingen, Germany, where he founded the Applied Rehabilitation Technology Lab to explore how to make novel technologies available to enable doctors to improve the lives of their patients.

### REFERENCES

- [1] A. M. Boudali, P. J. Sinclair, R. Smith, and I. R. Manchester, "Human locomotion analysis: Identifying a dynamic mapping between upper and lower limb joints using the Koopman operator," in *Proc. IEEE Int. Conf. Engineering in Medicine and Biology Society (EMBC)*, 2017, pp. 1889–1892. doi: 10.1109/EMBC.2017.8037216.
- [2] Össur. Accessed on: Mar. 24, 2020. [Online]. Available: <https://www.ossur.com/en-us/prosthetics/knees/mauch-knee>
- [3] "C-Leg above knee prosthetic leg," Otto Bock, Duderstadt, Germany. Accessed on: Mar. 24, 2020. [Online]. Available: <http://www.ottobockus.com/C-Leg.html>
- [4] Össur. Accessed on: Mar. 24, 2020. [Online]. Available: <https://www.ossur.com/en-us/prosthetics/knees/rheo-knee>

- [5] "Power knee," Össur, Reykjavík. Accessed on: Mar. 24, 2020. [Online]. Available: <https://www.ossur.com/en-us/prosthetics/knees/power-knee>
- [6] M. R. Tucker et al., "Control strategies for active lower extremity prosthetics and orthotics: A review," *J. Neuroeng. Rehabil.*, vol. 12, no. 1, pp. 1–29, 2015. doi: 10.1186/1743-0003-12-1.
- [7] D. Grimes, W. Flowers, and M. Donath, "Feasibility of an active control scheme for above knee prostheses," *Trans. ASME, J. Biomech. Eng.*, vol. 99, no. 4, pp. 215–221, 1977. doi: 10.1115/1.3426293.
- [8] D. L. Grimes, "An active multi-mode above knee prosthesis controller," Ph.D. dissertation, Massachusetts Inst. of Technol., Cambridge, 1979.
- [9] I. Jolliffe, *Principal Component Analysis*, 2nd ed. New York: Springer-Verlag, 2002.
- [10] H. Vallery, E. H. Van Asseldonk, M. Buss, and H. Van Der Kooij, "Reference trajectory generation for rehabilitation robots: Complementary limb motion estimation," *IEEE Trans. Neural Syst. Rehabil. Eng.*, vol. 17, no. 1, pp. 23–30, 2009. doi: 10.1109/TNSRE.2008.2008278.
- [11] F. Sup, A. Bohara, and M. Goldfarb, "Design and control of a powered transfemoral prosthesis," *Int. J. Robot. Res.*, vol. 27, no. 2, pp. 263–273, 2008. doi: 10.1177/0278364907084588.
- [12] B. E. Lawson, H. A. Varol, A. Huff, E. Erdemir, and M. Goldfarb, "Control of stair ascent and descent with a powered transfemoral prosthesis," *IEEE Trans. Neural Syst. Rehabil. Eng.*, vol. 21, no. 3, pp. 466–473, 2013. doi: 10.1109/TNSRE.2012.2225640.
- [13] E. J. Rouse, L. M. Mooney, and H. M. Herr, "Clutchable series-elastic actuator: Implications for prosthetic knee design," *Int. J. Robot. Res.*, vol. 33, no. 13, pp. 1611–1625, 2014. doi: 10.1177/0278364914545673.
- [14] D. Quintero, D. J. Villarreal, D. J. Lambert, S. Kapp, and R. D. Gregg, "Continuous-phase control of a powered knee–ankle prosthesis: Amputee experiments across speeds and inclines," *IEEE Trans. Robot.*, vol. 34, no. 3, pp. 686–701, 2018. doi: 10.1109/TRO.2018.2794536.
- [15] M. Holgate, T. Sugar, and A. Bohler, "A novel control algorithm for wearable robotics using phase plane invariants," in *Proc. IEEE Int. Conf. Robotics and Automation (ICRA)*, 2009, pp. 3845–3850. doi: 10.1109/ROBOT.2009.5152565.
- [16] H. Varol, F. Sup, and M. Goldfarb, "Real-time gait mode intent recognition of a powered knee and ankle prosthesis for standing and walking," in *Proc. IEEE RAS/EMBS Int. Conf. Biomedical Robotics and Biomechatronics (BioRob)*, 2008, pp. 66–72. doi: 10.1109/BIOROB.2008.4762860.
- [17] H. Varol, F. Sup, and M. Goldfarb, "Multiclass real-time intent recognition of a powered lower limb prosthesis," *IEEE Trans. Biomed. Eng.*, vol. 57, no. 3, pp. 542–551, 2010. doi: 10.1109/TBME.2009.2034734.
- [18] A. Kilicarslan, S. Prasad, R. G. Grossman, and J. L. Contreras-Vidal, "High accuracy decoding of user intentions using EEG to control a lower-body exoskeleton," in *Proc. Int. Conf. IEEE Engineering Medicine and Biology Society (EMBC)*, 2013, pp. 5606–5609. doi: 10.1109/EMBC.2013.6610821.
- [19] H. Huang, F. Zhang, L. J. Hargrove, Z. Dou, D. R. Rogers, and K. B. Englehart, "Continuous locomotion-mode identification for prosthetic legs based on neuromuscular–mechanical fusion," *IEEE Trans. Biomed. Eng.*, vol. 58, no. 10, pp. 2867–2875, 2011. doi: 10.1109/TBME.2011.2161671.
- [20] H. Huang, T. Kuiken, and R. Lipschutz, "A strategy for identifying locomotion modes using surface electromyography," *IEEE Trans. Biomed. Eng.*, vol. 56, no. 1, pp. 65–73, 2009. doi: 10.1109/TBME.2008.2003293.
- [21] D. Jin, J. Yang, R. Zhang, R. Wang, and J. Zhang, "Terrain identification for prosthetic knees based on electromyographic signal features," *Tsinghua Sci. Technol.*, vol. 11, no. 1, pp. 74–79, 2006. doi: 10.1016/S1007-0214(06)70157-2.
- [22] K. H. Ha, H. A. Varol, and M. Goldfarb, "Volitional control of a prosthetic knee using surface electromyography," *IEEE Trans. Biomed. Eng.*, vol. 58, no. 1, pp. 144–151, 2011. doi: 10.1109/TBME.2010.2070840.
- [23] A. J. Young, A. M. Simon, N. P. Fey, and L. J. Hargrove, "Intent recognition in a powered lower limb prosthesis using time history information," *Ann. Biomed. Eng.*, vol. 42, no. 3, pp. 631–641, 2014. doi: 10.1007/s10439-013-0909-0.
- [24] A. Young, T. Kuiken, and L. Hargrove, "Analysis of using EMG and mechanical sensors to enhance intent recognition in powered lower limb prostheses," *J. Neural Eng.*, vol. 11, no. 5, p. 056021, 2014. doi: 10.1088/1741-2560/11/5/056021.
- [25] A. J. Young, A. M. Simon, N. P. Fey, and L. J. Hargrove, "Classifying the intent of novel users during human locomotion using powered lower limb prostheses," in *Proc. Int. IEEE/EMBS Conf. Neural Engineering (NER)*, 2013, pp. 311–314. doi: 10.1109/NER.2013.6695934.
- [26] H. Varol and M. Goldfarb, "Real-time intent recognition for a powered knee and ankle transfemoral prosthesis," in *Proc. IEEE Int. Conf. Rehabilitation Robotics (ICORR)*, 2007, pp. 16–23. doi: 10.1109/ICORR.2007.4428400.
- [27] L. Wang, E. H. van Asseldonk, and H. van der Kooij, "Model predictive control-based gait pattern generation for wearable exoskeletons," in *Proc. IEEE Int. Conf. Rehabilitation Robotics (ICORR)*, 2011, pp. 1–6. doi: 10.1109/ICORR.2011.5975442.
- [28] H. L. Bartlett and M. Goldfarb, "A phase variable approach for IMU-based locomotion activity recognition," *IEEE Trans. Biomed. Eng.*, vol. 65, no. 6, pp. 1330–1338, 2018. doi: 10.1109/TBME.2017.2750139.
- [29] D. J. Villarreal, H. A. Poonawala, and R. D. Gregg, "A robust parameterization of human gait patterns across phase-shifting perturbations," *IEEE Trans. Neural Syst. Rehabil. Eng.*, vol. 25, no. 3, pp. 265–278, 2017. doi: 10.1109/TNSRE.2016.2569019.
- [30] C. E. Rasmussen and C. K. I. Williams, *Gaussian Processes for Machine Learning*. Cambridge, MA: MIT Press, 2006.
- [31] M. Xiloyannis, C. Gavriel, A. A. Thomik, and A. A. Faisa, "Gaussian process regression for accurate prediction of prosthetic limb movements from the natural kinematics of intact limbs," in *Proc. IEEE/EMBS Int. Conf. Neural Engineering*, 2015, pp. 659–662. doi: 10.1109/NER.2015.7146709.
- [32] Y. Yun, H.-C. Kim, S. Y. Shin, J. Lee, A. D. Deshpande, and C. Kim, "Statistical method for prediction of gait kinematics with Gaussian process regression," *J. Biomed. Eng.*, vol. 47, no. 1, pp. 186–192, 2014. doi: 10.1016/j.jbiomech.2013.09.032.
- [33] N. Mathur, I. Glesk, and A. Buis, "Skin temperature prediction in lower limb prostheses," *IEEE J. Biomed. Health Inform.*, vol. 20, no. 1, pp. 158–165, 2016. doi: 10.1109/JBHI.2014.2368774.
- [34] N. Dhir, H. Dallali, E. M. Ficanha, G. A. Ribeiro, and M. Rastgaard, "Locomotion envelopes for adaptive control of powered ankle prostheses," in *Proc. IEEE Int. Conf. Robotics and Automation (ICRA)*, 2018, pp. 1488–1495. doi: 10.1109/ICRA.2018.8460929.
- [35] M. Grimmer and A. Seyfarth, "Stiffness adjustment of a series elastic actuator in a knee prosthesis for walking and running: The trade-off between energy and peak power optimization," in *Proc. IEEE Int. Conf. Intelligent Robots and Systems (IROS)*, 2011, pp. 1811–1816. doi: 10.1109/IROS.2011.6094467.
- [36] F. Sup, H. A. Varol, J. Mitchell, T. Withrow, and M. Goldfarb, "Design and control of an active electrical knee and ankle prosthesis," in *Proc. IEEE RAS/EMBS Int. Conf. Biomedical Robotics and Biomechatronics (BioRob)*, 2008, pp. 523–528. doi: 10.1109/BIOROB.2008.4762811.
- [37] P. Scholl, V. Grabosch, M. Eslamy, and A. Seyfarth, "Comparison of peak power and energy requirements in different actuation concepts for active knee prosthesis," in *Proc. IEEE Int. Conf. Mechatronics and Automation*, 2015, pp. 1448–1453. doi: 10.1109/ICMA.2015.7237698.
- [38] M. Grimmer, M. Eslamy, S. Gliech, and A. Seyfarth, "A comparison of parallel- and series elastic elements in an actuator for mimicking human ankle joint in walking and running," in *Proc. IEEE Int. Conf. Robotics and Automation (ICRA)*, 2012, pp. 2463–2470. doi: 10.1109/ICRA.2012.6224967.
- [39] M. Eslamy, M. Grimmer, and A. Seyfarth, "Effects of unidirectional parallel springs on required peak power and energy in powered prosthetic ankles: Comparison between different active actuation concepts," in *Proc. IEEE Int. Conf. Robotics and Biomimetics*, 2012, pp. 2406–2412. doi: 10.1109/ROBIO.2012.6491330.
- [40] M. Eslamy, M. Grimmer, S. Rinderknecht, and A. Seyfarth, "Does it pay to have a damper in a powered ankle prosthesis? A power-energy perspective," in *Proc. IEEE Int. Conf. Rehabilitation Robotics (ICORR)*, 2013, pp. 1–8. doi: 10.1109/ICORR.2013.6650562.
- [41] S. Lipfert, *Kinematic and Dynamic Similarities Between Walking and Running*. Hamburg: Verlag Dr. Kovac, 2010.
- [42] M. W. Whittle, *Gait Analysis: An Introduction*. Oxford, U.K.: Butterworth-Heinemann, 2003.
- [43] C. E. Rasmussen and C. K. I. Williams, *Gaussian Processes for Machine Learning*. Cambridge, MA: MIT Press, 2006. [Online]. Available: <http://www.gaussianprocess.org/gpml>
- [44] A. Findlow, J. Goulermas, C. Nester, D. Howard, and L. Kenney, "Predicting lower limb joint kinematics using wearable motion sensors," *Gait Posture*, vol. 28, no. 1, pp. 120–126, 2008. doi: 10.1016/j.gaitpost.2007.11.001.
- [45] J. Goulermas, D. Howard, C. Nester, R. Jones, and L. Ren, "Regression techniques for the prediction of lower limb kinematics," *J. Biomed. Eng.*, vol. 127, no. 6, pp. 1020–1024, 2005. doi: 10.1115/1.2049328.
- [46] R. A. Bogey and L. A. Barnes, "An EMG-to-force processing approach for estimating in vivo hip muscle forces in normal human walking," *IEEE Trans. Neural Syst. Rehabil. Eng.*, vol. 25, no. 8, pp. 1172–1179, 2017. doi: 10.1109/TNSRE.2016.2613021.